

Subthalamic and pallidal oscillations and their couplings reflect dystonia severity and improvements by deep brain stimulation

Xinyi Geng^{a,b,c,*}, Zhaoyu Quan^d, Ruili Zhang^{a,e}, Guanyu Zhu^f, Yingnan Nie^{a,e}, Shouyan Wang^{a,e}, Edmund Rolls^{a,g}, Jianguo Zhang^{f,**}, Li Hu^{b,c}

^a Institute of Science and Technology for Brain-Inspired Intelligence, Fudan University, Shanghai, China

^b CAS Key Laboratory of Mental Health, Institute of Psychology, Chinese Academy of Sciences, Beijing, China

^c Department of Psychology, University of Chinese Academy of Sciences, Beijing, China

^d Academy for Engineering and Technology, Fudan University, Shanghai, China

^e Key Laboratory of Computational Neuroscience and Brain-Inspired Intelligence (Fudan University), Ministry of Education, China

^f Department of Neurosurgery, Beijing Tian-Tan Hospital, Beijing Neurosurgical Institute, Capital Medical University, China

^g Oxford Centre for Computational Neuroscience, University of Oxford, Oxford, UK

ARTICLE INFO

Keywords:

Subthalamic nucleus
Globus pallidus internus
Dystonia
Oscillations and couplings
Deep brain stimulation

ABSTRACT

Background: Deep brain stimulation (DBS) targeting the globus pallidus internus (GPI) and subthalamic nucleus (STN) is employed for the treatment of dystonia. Pallidal low-frequency oscillations have been proposed as a pathophysiological marker for dystonia. However, the role of subthalamic oscillations and STN-GPI coupling in relation to dystonia remains unclear.

Objective: We aimed to explore oscillatory activities within the STN-GPI circuit and their correlation with the severity of dystonia and efficacy achieved by DBS treatment.

Methods: Local field potentials were recorded simultaneously from the STN and GPI from 13 dystonia patients. Spectral power analysis was conducted for selected frequency bands from both nuclei, while power correlation and the weighted phase lag index were used to evaluate power and phase couplings between these two nuclei, respectively. These features were incorporated into generalized linear models to assess their associations with dystonia severity and DBS efficacy.

Results: The results revealed that pallidal theta power, subthalamic beta power and subthalamic-pallidal theta phase coupling and beta power coupling all correlated with clinical severity. The model incorporating all selected features predicts empirical clinical scores and DBS-induced improvements, whereas the model relying solely on pallidal theta power failed to demonstrate significant correlations.

Conclusions: Beyond pallidal theta power, subthalamic beta power, STN-GPI couplings in theta and beta bands, play a crucial role in understanding the pathophysiological mechanism of dystonia and developing optimal strategies for DBS.

1. Introduction

Dystonia is a movement disorder characterized by abnormal sustained or intermittent muscle contractions (Albanese et al., 2013). Nuclei in the basal ganglia, which are crucial for sensorimotor control, are targeted in deep brain stimulation (DBS) treatment for segmental and generalized dystonia, specifically the globus pallidus internus (GPI)

(Albanese, 2014; Romito et al., 2013). While the pathological mechanism of dystonia remains unclear, research suggests that low activation of the GPI diminishes its inhibitory effect on the thalamus, leading to increased cortical excitability and hyperkinetic symptoms (Neumann et al., 2017; Marsden and Obeso, 1994). This is supported by accumulating evidence that pallidal oscillatory activity in the low-frequency band (4–12 Hz) is prominent (Neumann et al., 2019; Lopez-Azcarate

* Correspondence to: Xinyi Geng, CAS Key Laboratory of Mental Health, Institute of Psychology, Chinese Academy of Sciences, 16 Yard of Lincui Rd, Chaoyang District, Beijing, China.

** Correspondence to: Jianguo Zhang, Department of Neurosurgery, Beijing Tian-Tan Hospital, Beijing Neurosurgical Institute, Capital Medical University, 119 West of the South Fourth Ring Road, Fengtai District, China.

E-mail addresses: gengxinyi@fudan.edu.cn (X. Geng), Zjguo73@126.com (J. Zhang).

<https://doi.org/10.1016/j.nbd.2024.106581>

Received 19 April 2024; Received in revised form 5 June 2024; Accepted 25 June 2024

Available online 25 June 2024

0969-9961/© 2024 The Authors. Published by Elsevier Inc. This is an open access article under the CC BY-NC license (<http://creativecommons.org/licenses/by-nc/4.0/>).

et al., 2010; Lee and Kiss, 2014; Pina-Fuentes et al., 2018; Pina-Fuentes et al., 2020) and correlated with symptom severity across multiple dystonia types (Neumann et al., 2017; Scheller et al., 2019a). Although the GPi remains the primary stimulating target, the subthalamic nucleus (STN) has also shown promise in treating cranial, cervical and generalized dystonia (Ostrem et al., 2011; Schjerling et al., 2013; Xie et al., 2024). A recent study highlighted dysfunctional networks in dystonia, emphasizing interconnections between the STN and the sensorimotor cortices (Hollunder et al., 2024). However, compared to findings on pallidal low-frequency oscillations, observations regarding the STN remain inconclusive (Wang et al., 2016; Geng et al., 2017; Wiest et al., 2023).

In addition, several studies have reported increased beta activity in the GPi and STN in dystonia patients with drug-induced dopamine deficiency (Geng et al., 2017; Scheller et al., 2019b; Weinberger et al., 2012; Kuehn et al., 2008). Beta oscillation (12–32 Hz) is commonly observed in the basal ganglia nuclei in Parkinson's disease (PD) patients and reflects hypokinetic movements. It has been suggested that subcortical beta oscillation represents a symptom-specific marker of slow movement, which increases with DBS-induced bradykinesia in dystonia (Lofredi et al., 2023). The synchronization level within the beta band is considered a crucial factor in gating information in the cortico-basal ganglia circuit, and any exaggerated or excessively suppressed abnormality can lead to motor impairments (Brittain and Brown, 2014; Chen et al., 2006). A study examining phase alignment between the STN and GPi in PD patients revealed that increased beta power correlates with the duration of beta-amplifying phase alignment between the two nuclei, and that dopaminergic medication led to reduced phase locking value (Cagnan et al., 2015). However, it remains unclear whether beta synchronization exists within the local STN-GPi circuit in dystonia, and whether it is associated with the symptoms in dystonia.

Given the significant interplay between the STN and GPi in the cortico-basal ganglia circuit for motor control, and the fact that both nuclei have been used as potential DBS target for treating dystonia, we hypothesize that oscillatory activities, as well as the connectivity between the two nuclei could reflect the symptomatic severity of dystonia. In this study, we investigated the oscillatory power, phase coupling, and power coupling of local field potentials (LFPs) recorded simultaneously from the two nuclei, and evaluated their associations with dystonia severity and DBS efficacy.

Table 1
Summary of clinical information and data.

| Case | Sex | Age/ Duration (year) | Diagnose & Dominated symptoms | History of medication treatment | Clinical scales BFMDRS (MS*) (Pre-op/ post-op) | Nuclei as final target for DBS |
|------|-----|----------------------------|--|--|---|-----------------------------------|
| 1 | F | 65/5 | Cranial / Blepharospasm, frowning, bruxism, laryngismus, breathing difficulty | None | 16/5 | GPi |
| 2 | F | 49/3 | Cranial & Cervical / Blepharospasm, displaced jaw, back head stiffness, phasic head movement (left and right) | Clonazepam, Baclofen, Artane, Haloperidol, | 16/8 | GPi |
| 3 | F | 57/5 | Cranial / Blepharospasm, lip tightening, mild discomfort on shoulders | None | 11/3 | STN |
| 4 | M | 40/3 | Cervical & Gait disorder / Retrocollis (right) and laterocollis (left), right lower limb stiffness and pain | None | 22/16 | GPi |
| 5 | F | 59/2 | Cervical & Gait disorder / Phasic head movement (back and forth), dysarthria, dysphagia, left lower limb stiffness | None | 27/8 | GPi |
| 6 | M | 70/1 | Cranial / Blepharospasm, oromandibular spasm, anterocollis (right) | Baclofen, Eperisone hydrochloride | 15.5/6 | GPi |
| 7 | M | 53/1 | Cranial / Blepharospasm | Baclofen | 12/8 | STN |
| 8 | F | 68/1 | Cranial / Blepharospasm, trismus, dysphagia | None | 29/NA | NA |
| 9 | F | 63/7 | Cervical / Laterocollis (left), stiffness on left upper limb and right trapezius and levator scapulae | None | 24/6 | GPi |
| 10 | F | 34/8 | Generalized / Retrocollis (left), tilting trunk (left), erector spinae tremor, gait disorder | Clonazepam, Baclofen, Artane | 36/8 | GPi |
| 11 | F | 49/1 | Cranial / Blepharospasm, frowning, oromandibular spasm, bruxism | None | 18/6 | GPi |
| 12 | M | 60/2 | Cervical / Laterocollis (left) | None | 22/NA | GPi |
| 13 | F | 76/5 | Cervical / Laterocollis (right) | None | 40/26 | GPi |

BFMDRS(MS): Burke-Fahn-Marsden Dystonia Rating Scale, Motor Scales. Pre-op: pre-operative; Post-op: post-operative.

2. Methods

2.1. Subjects and materials

Thirteen patients (9 females, aged 57.15 ± 11.99 (mean \pm SD) years) with cranial, cervical, and generalized primary dystonia underwent DBS electrode implantation at Beijing Tian-Tan Hospital, Capital Medical University, Beijing. Patients with secondary dystonia and cerebral palsy were excluded in this study. All patients provided written informed consent to participate in this study, which was approved by the local ethics committee (No. KY2016–038-02). Twelve patients underwent bilateral STN and GPi implantation. One patient underwent unilateral STN and bilateral GPi implantation. Ultimately, based on the temporary stimulation effects post-surgery and the brain imaging information of the implanted electrodes, one pair of electrodes either in the STN or GPi was selected as the final target for DBS, and the implanted electrodes from the other nucleus were removed. All patients underwent clinical evaluation using the motor scale of the Burke-Fahn-Marsden Dystonia Rating Scale (BFMDRS) before and 3–6 months after surgery (Muller et al., 2004; Susatia et al., 2010). The clinical details are given in Table 1. The clinical improvement was calculated as follows:

$$\text{Improvement} = \frac{|BFMDRS_{\text{postoperative}} - BFMDRS_{\text{preoperative}}|}{BFMDRS_{\text{preoperative}}} \times 100\%$$

The procedures for STN and GPi targeting, and DBS electrode implantation have been previously reported (Geng et al., 2017; Chou et al., 2005). Specifically, the electrodes were targeted to the dorsolateral area of the STN and the posteroventral-lateral part of GPi. The DBS electrodes used were PINS L301 for STN and L302 for GPi (PINS, Beijing, China) with four platinum-iridium cylindrical surface contacts. Each contact was 1.27 mm in diameter and 1.5 mm in length and was separated by 0.5 mm for module L301 and 1.5 mm for module L302. The most caudal contact is named contact 0, and the most rostral contact is named contact 3. The placement of DBS electrodes was confirmed with fused postoperative and preoperative magnetic resonance images.

2.2. LFP recordings and signal processing

All patients underwent recordings of LFPs from externalized electrode leads 3–5 days following surgery. Patients were not instructed to

suppress any involuntary movements but were instructed to avoid voluntary movements during the recording. The patients sat at rest without external support for 30 min. The temporary DBS was switched off for at least 5 h before the recording. In all patients, bipolar LFPs were recorded from the adjacent contacts (contact pairs: 0–1, 1–2, 2–3) of each DBS electrode. The signals were amplified with a gain of 24, bandpass filtered over 1–250 Hz and recorded with a sampling frequency of 500 Hz using customized wireless amplifiers (Zhang et al., 2020). One channel of LFPs was respectively selected from each nucleus for analyses based on the location of the contacts.

Signal processing, data analysis, statistical analysis and figure illustration were performed offline with scripts developed in MATLAB (MathWorks Inc.). LFPs were bandpass filtered over 2–90 Hz with a Chebyshev Type I filter and line noise was removed with a notch filter. The signals were partitioned into multiple segments, each with a duration of 20 s. The segments with large artifacts that met the criteria: $\bar{s}_{\text{seg}} > \bar{s} + 3\text{SD}$ (where \bar{s}_{seg} represents the mean of the selected segment, and \bar{s} and SD respectively represent the mean and the standard deviation of the total signal) were rejected from all channels. Approximately, 25 min of artifact-free signal from each nucleus was used for further analyses.

To determine the frequency bands to investigate, we first calculated the power spectral density (PSD) of subthalamic and pallidal LFPs based on Welch's method (Welch, 1967) with a 1 s sliding-window, 75% overlap and 2048 points. The PSDs were then correlated with the motor scale of the BFMDRS at each frequency point (shown in Fig. 1). The frequency bands were categorized into the following ranges: 4–8 Hz, 8–12 Hz, 12–16 Hz, 16–20 Hz, 20–24 Hz, 24–32 Hz, 32–44 Hz and 54–90 Hz. If adjacent bands consistently exhibited correlations with the scores, they were merged into a single band for subsequent analysis.

2.3. Feature extraction

We calculated the auto-spectra and cross-spectra of the time-aligned segments from the STN and GPi using a short-time Fourier transform with a 1 s sliding window, 90% overlap and 2048 points. The power-based and phase-based features were extracted from the time-frequency spectrograms and averaged across segments.

The spectral powers of subthalamic and pallidal LFPs were averaged over the designated frequency bands, resulting in two matrices each with a size of 25×8 (sides \times bands). Notably, the pallidal band power of case 10 was included for feature selection but excluded for model fitting

due to inconsistencies in the length of the model input data.

Power coupling between the ipsilateral STN and GPi was estimated through power correlation in the time-frequency domain. It correlates the time series of band-averaged power of the STN and GPi within the same frequency bands. The value between frequency bands i of the STN ($Pw_{x,i}$) and GPi ($Pw_{y,i}$) is given as:

$$XCor_{xy} = \text{corr}(Pw_{x,i}, Pw_{y,i})$$

where Pw_i represents the averaged power time series of the i th frequency band and corr represents Pearson's correlation.

The phase coupling was estimated by the weighted phase lag index (wPLI). It quantifies the overall directionality of phase angle differences between a pair of signals (Vinck et al., 2011; Cohen, 2014). A high wPLI indicates a tendency for phase angle differences between the STN and GPi to cluster on either the positive or negative side of the imaginary axis with weighting on the real axis, suggesting high phase-locking between the two nuclei at a specific frequency. The wPLI between two time series $x(t)$ and $y(t)$ at frequency f is given by:

$$wPLI_{xy}(f) = \frac{n^{-1} \sum_{t=1}^n |\text{imag}[S_{xy}(f)]| \text{sgn}[\text{imag}[S_{xy}(f)]]}{n^{-1} \sum_{t=1}^n |\text{imag}[S_{xy}(f)]|}$$

where $S_{xy}(f)$ represents the cross-spectrum of the signals at frequency f , $\text{imag}[\cdot]$ represents the imaginary part of the spectrum and $\text{sgn}[\cdot]$ means keeping the sign (+ / -) for the part in parentheses.

Consequently, four matrices of size 25×8 were extracted to represent spectral power of two nuclei, as well as power-based and phase coupling between two nuclei (shown in Fig. 2).

2.4. Generalized linear model (GLM)

GLM was used to assess the potential contributions of selected features in predicting the clinical severity of dystonia. GLM represents a broad extension of linear model, specifically tailored to handle non-normal distributions of variables. By preserving the inherent measurement properties of data, GLM effectively accommodates nonlinearities and heteroscedasticity within the data structure.

Features for model fitting were selected based on the correlation coefficients and P -values of correlations between the specific feature and clinical severity. Accordingly, six features were chosen as the input for the GLM: subthalamic spectral power over 8–12 Hz and 16–24 Hz,

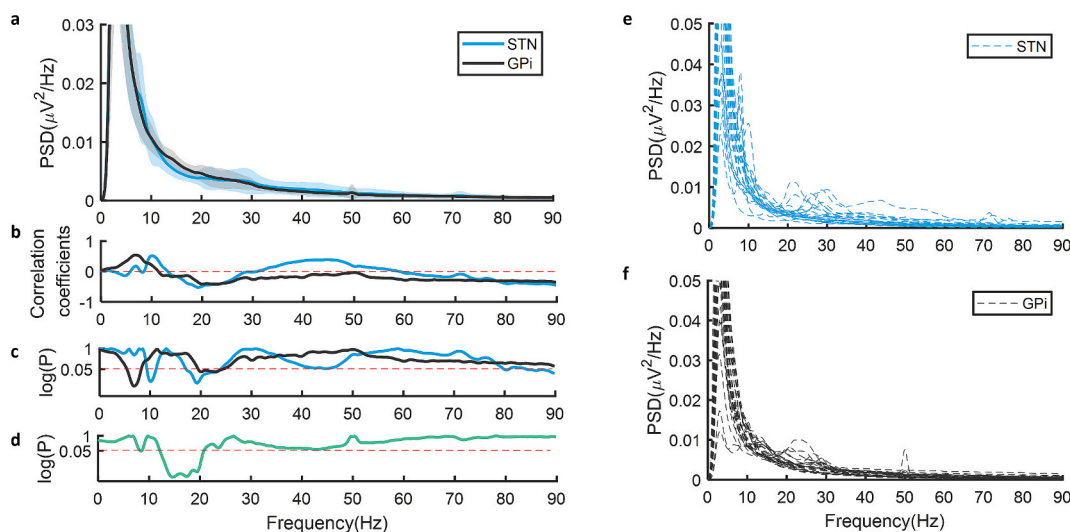


Fig. 1. Overview of oscillatory power and correlations with clinical scores. (a) PSD of LFPs in the STN (blue line) and GPi (black line), in which the shadows represent \pm SD. (b) Correlation coefficients of correlations between clinical scores and PSDs in the STN and GPi. (c) The corresponding logarithm of P -values of correlations. (d) The logarithm of P -values of the paired t -test comparing the PSDs between the STN and GPi. (e-f) The individual PSDs of the STN (blue dash lines) and GPi (black dash lines). (For interpretation of the references to colour in this figure legend, the reader is referred to the web version of this article.)

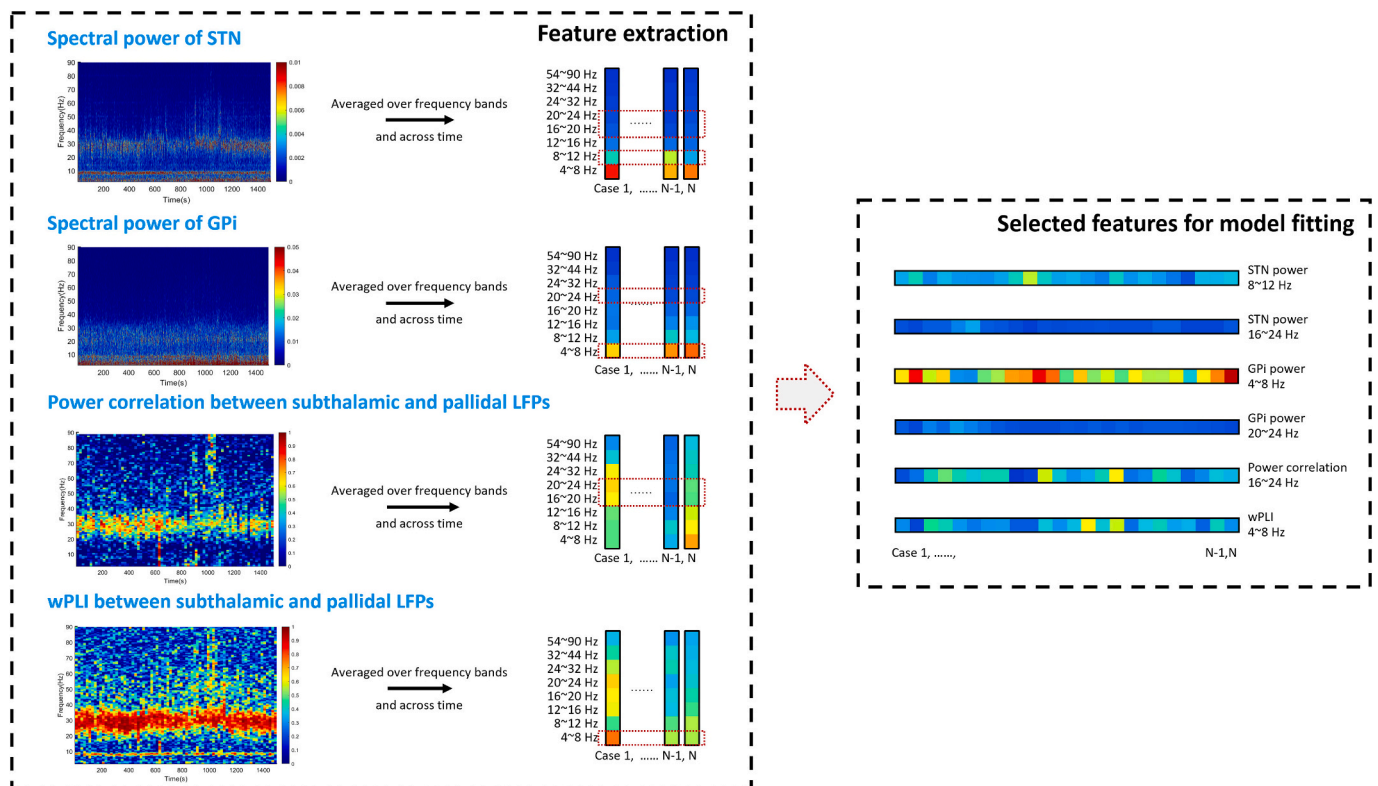


Fig. 2. Processes for feature extraction and selection. Spectral power, power correlation and wPLI were calculated over 20 s epochs and averaged across time. All features are then binned into eight frequency bands. Six features were selected for model fitting based on their clinical correlations, each of which was a $N \times 1$ ($N = 25$) vector that represented spectral power or couplings over a certain frequency band.

pallidal spectral power over 4–8 Hz and 20–24 Hz, STN-GPi power correlation over 16–24 Hz and wPLI over 4–8 Hz. All features underwent z-score normalization before being fitted into GLMs using the MATLAB function fitglm. The optimal GLM was determined using the maximum likelihood estimation between the empirical and model-estimated data. Additionally, the model was fitted with solely the pallidal theta power for comparison. The same set of features was also used to assess their ability to estimate the clinical improvements achieved by DBS.

2.5. Statistical analysis

The clinical scores and improvements were duplicated for both hemisphere to meet the sample size of LFPs for analyses (Benjamini and Hochberg, 2018). Pearson's correlation was applied to evaluate the relationship between oscillatory activities and the clinical severity of dystonia. The P -values in the correlation analysis were corrected using the false discovery rate (FDR) for multiple comparisons. Features with corrected P -values below 0.05 were considered significantly correlated with clinical severity. The GLM generated coefficient estimates (b_i , $i \in [0, 6]$) for the input features and P -values for the hypothesis that the corresponding coefficient would be zero or not. Coefficients with P -values below 0.05 were deemed significantly associated with clinical severity. Additionally, the coefficient of determination (R^2) evaluated the explanatory power of the model. A Chi-square (χ^2) test assessed whether the model significantly improved fit compared to a constant-only model.

3. Results

In our patient cohort, the preoperative BFMDRS (motor part) was 22.19 ± 8.89 (mean \pm SD) and the average improvement of DBS treatment was $58.02 \pm 18.43\%$. The LFPs revealed prominent peaks in the broad band over 4–12 Hz in 17 hemispheres of the STN and 21

hemispheres of the GPi by visual inspection. Notably, 11 sides of both the STN and GPi also showed distinct power peaks in the beta frequency band (12–32 Hz), with 4/11 sides recorded in patients who had history of medication treatment. Additionally, fine-tuned gamma activity around 70–80 Hz was detected on 4 sides of the STN in 3 patients. Significant difference in PSDs of the STN and GPi were observed around 8.5 Hz and 42 Hz, and over 12–20 Hz frequency band (Fig. 1d).

3.1. Low-frequency and beta oscillations in the STN and GPi exhibit distinct clinical correlations

Consistent with and expanding on findings in previous studies, our results demonstrated positive correlations between low-frequency oscillations and clinical scores in both the GPi and STN, albeit within distinct frequency bands. Specifically, as illustrated in Fig. 3a-d, subthalamic alpha power over 8–12 Hz ($N = 25$, $P_{FDR} = 0.019$) and pallidal theta power over 4–8 Hz ($N = 26$, $P_{FDR} = 0.011$) had positive correlations with clinical severity. In contrast to earlier research (Neumann et al., 2017) indicating no correlation between pallidal beta power and dystonic severity, our data revealed a negative correlation for pallidal beta power over 20–24 Hz ($N = 26$, $P_{FDR} = 0.013$). Similarly, for the STN, negative correlations were found between the spectral power over 16–24 Hz and clinical scores ($N = 25$, $P_{FDR} = 0.023$).

3.2. Couplings between the STN and GPi are negatively correlated with clinical severity

As illustrated in Fig. 3, a negative correlation was observed between the phase coupling measured by wPLI over 4–8 Hz and clinical severity ($N = 25$, $P_{FDR} = 0.015$). The power coupling in the beta band at 16–24 Hz revealed a significant negative correlation with clinical severity ($N = 25$, $P_{FDR} = 0.014$). The significant frequency band for correlations between pallidal power and clinical scores has been identified in the range

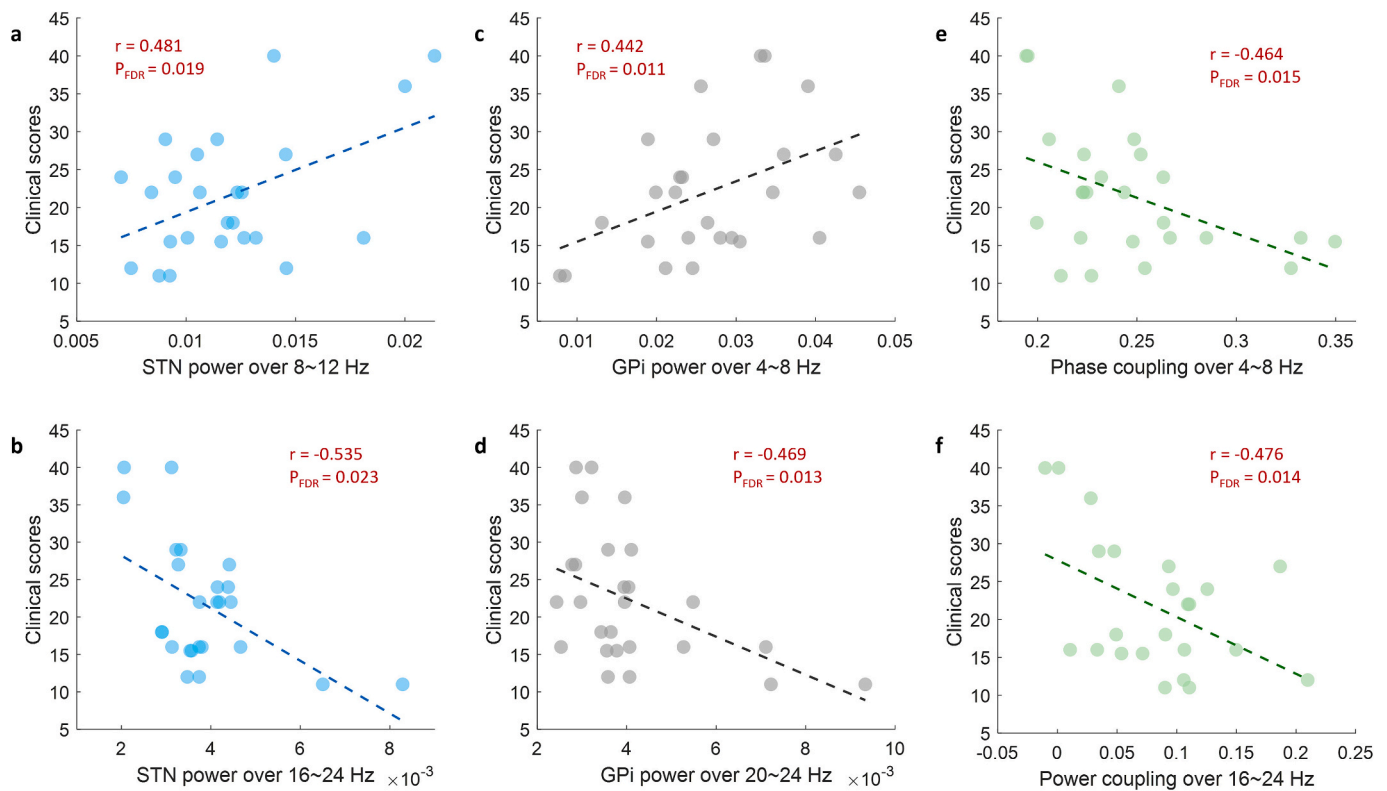


Fig. 3. Correlations between selected oscillatory features and clinical scores. (a) Correlation between subthalamic power over 8–12 Hz and clinical scores; (b) Correlation between subthalamic power over 16–24 Hz and clinical scores; (c) Correlation between pallidal power over 4–8 Hz and clinical scores; (d) Correlation between pallidal power over 20–24 Hz and clinical scores; (e) Correlation between subthalamic-pallidal phase coupling over 4–8 Hz and clinical scores; (f) Correlation between subthalamic-pallidal power coupling over 16–24 Hz and clinical scores. P-values shown in the panels are FDR corrected. Significant positive correlations were found between clinical scores and STN alpha power and GPI theta power, while significant negative correlations were found between clinical scores and beta power in both nuclei, as well as between clinical scores and STN-GPI couplings.

of 4–8 Hz; while correlations between subthalamic power and clinical scores have been observed in the range of 16–24 Hz. The concordance of similarities in these frequency ranges underscores the significance of the GPI in theta phase-locking and the STN in beta power synchronization.

3.3. Contributions of oscillatory activities and couplings to clinical severity and DBS improvements

Having identified the features with a significant clinical correlation, we proceeded to assess their associations with the severity of symptoms in dystonia. A GLM with a Poisson distribution was fitted to six selected features as follows:

$$y \sim b_0 + b_1x_1 + b_2x_2 + b_3x_3 + b_4x_4 + b_5x_5 + b_6x_6$$

The coefficient of determination (R^2) was 0.504, indicating that the model explained 50.4% of the variability in clinical scores. The χ^2 test for the model was 68.7 and $P = 7.45 \times 10^{-13}$, demonstrating adequate model fit. As shown in Fig. 4a, the empirical clinical scores and the model-estimated clinical scores were significantly correlated ($r = 0.816$, $P = 6.45 \times 10^{-7}$). Ordering the absolute values of b_i from largest to smallest yields the four features that significantly contribute to the dependent variable y (clinical scores) of the model: pallidal theta power ($b = 2.972$, $P = 0.039$), theta phase coupling ($b = -2.958$, $P = 0.01$), subthalamic beta power ($b = -2.846$, $P = 0.018$) and beta power coupling ($b = -2.736$, $P = 0.032$).

Using the same set of features as independent variables and DBS improvements as dependent variables in a GLM, the results indicate that these features can also reflect the improvement of DBS treatment (model $R^2 = 0.286$, $\chi^2 = 33.1$, $P = 1 \times 10^{-5}$). A significant linear correlation was also observed between the empirical DBS improvements and the model-

estimated data ($r = 0.534$, $P = 0.013$; shown in Fig. 4c).

Additionally, Fig. 4 shows that there was no significant correlation between the empirical clinical scores and model-estimated data solely using pallidal theta power. This suggests that the pallidal theta power can only explain a portion of the information to predict clinical scores (model $R^2 = 0.152$) and DBS-induced improvements (model $R^2 = 0.002$).

4. Discussion

Here we present simultaneous recorded oscillatory activities and cross-nucleus couplings within the STN-GPI circuit in dystonia patients. Our findings revealed significant associations between dystonic severity and pallidal theta power, subthalamic beta power, theta phase coupling, and beta power coupling. Crucially, the clinical scores and improvements estimated by the model with six selected features as predictors exhibited stronger linear correlations with the empirical data compared to those derived solely from pallidal theta oscillation. This underscores the importance of concurrently utilizing theta and beta oscillations, along with their couplings in the STN-GPI circuit, in elucidating the pathophysiological mechanisms of dystonia and offers valuable insights for developing strategies for subthalamic and pallidal DBS. In addition, while there is positive correlation between GPI theta and dystonia symptoms, the correlation between beta and dystonia symptoms are negative. This provides further evidence for the ‘hypokinetic’ role of beta oscillations cross disorders.

4.1. Low-frequency oscillations in dystonia

Low-frequency oscillations in the basal ganglia have been reported as

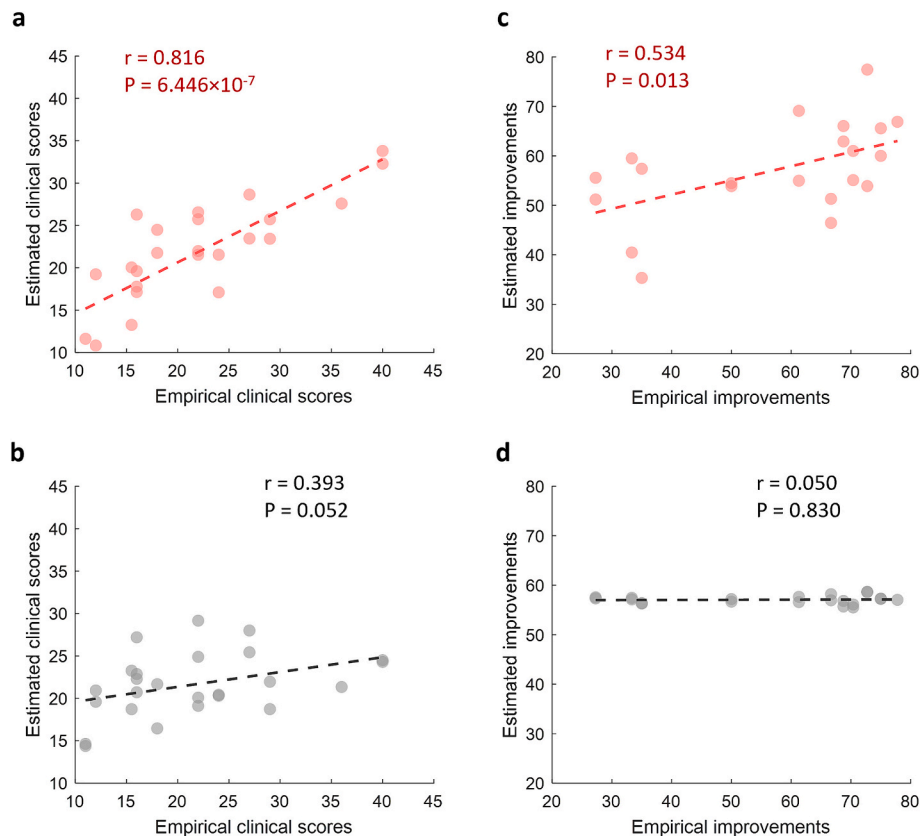


Fig. 4. Correlations between the empirical clinical scores and DBS improvements and their respective model-estimated data. (a) Correlations between the empirical preoperative clinical scores and the clinical scores estimated by the model fitted with six features, i.e. subthalamic power over 8–12 Hz and 16–24 Hz, pallidal power over 4–8 Hz and 20–24 Hz, power coupling over 16–24 Hz and phase coupling over 4–8 Hz. The model-estimated data is highly correlated with the empirical clinical scores. (b) No significant correlation between the empirical preoperative clinical scores and the data estimated by the model fitted with pallidal power over 4–8 Hz only. (c) Significant correlation between the empirical DBS improvements and data estimated by the model fitted with the six features listed above. (d) No significant correlation between the empirical DBS improvements and data estimated by the model fitted solely with pallidal power over 4–8 Hz.

symptom-specific in hyperkinetic disorders (Geng et al., 2017; Chen et al., 2006; Zhu et al., 2018), including dystonia, with studies indicating their potential to disrupt physiological motor function and induce dystonic muscle contractions. In light of this, previous studies revealed elevated low-frequency oscillatory power in the presence of abnormal muscle contractions (Zhang et al., 2023) and its association with prolonged dystonic movements (Liu et al., 2006). Moreover, previous studies revealed a positive correlation between interhemispheric pallidal low-frequency coherence and clinical severity in cervical dystonia (Neumann et al., 2017; Moll et al., 2014). Low-frequency coherence between the GPi and GPe (externus) has also been reported but shown no clinical correlation (Yokochi et al., 2018).

In this study, we provide further evidence linking low-frequency oscillations in the basal ganglia to the symptomatic severity of dystonia. Specifically, we observed a positive clinical correlation with the spectral power of low-frequency oscillations, particularly in the theta (4–8 Hz) band in the GPi and the alpha (8–12 Hz) band in the STN. However, our findings also suggest that while pallidal theta power contributes significantly to clinical scores, it alone could not fully explain dystonic severity. This is evident in the lack of correlation between empirical clinical scores and the model-estimated data when using solely the pallidal theta power in the model. These results imply that additional factors beyond pallidal theta oscillation may play a role in determining dystonic severity.

4.2. Beta oscillations in dystonia

In addition to theta oscillations, beta activities in the basal ganglia

are importantly involved in pathological and physiological motor control (Brittain and Brown, 2014; Brittain et al., 2014). Excessive increases and decreases in beta power can cause circuit imbalances and lead to motor impairments (Brittain and Brown, 2014). Over-synchronized beta activities in the basal ganglia have been widely discussed in PD as a biomarker of hypokinetic symptoms (Brittain et al., 2014). Recently, a study suggested that pallidal beta oscillations represent a symptom-specific activity of movement slowness, which increases with DBS-induced bradykinesia in dystonia (Lofredi et al., 2023). In this study, we observed a negative correlation between clinical scores and beta oscillations in both the STN and GPi. The GLM also revealed a strong association between subthalamic beta power and dystonic severity, indicating that lack of subthalamic beta oscillations is implicated in dystonic movements, contrasting with PD (Brittain et al., 2014). It is noteworthy that low-beta and high-beta oscillations have been extensively discussed in the context of PD, wherein levodopa can selectively modulate low-beta power. However, in dystonia studies, the differentiation between low-beta and high-beta is not as evident as it is in PD (Pina-Fuentes et al., 2018; Wang et al., 2016; Barow et al., 2014). In this study, the subthalamic beta power and beta power coupling within the 16–20 Hz and 20–24 Hz ranges consistently correlated with clinical scores, leading us to merge them into a unified 16–24 Hz band.

Although increased beta activity in the GPi and STN has been reported in dystonia patients with drug-induced dopamine deficiency (Geng et al., 2017; Kuehn et al., 2008), we noted prominent beta peaks in these nuclei in patients who had withdrawn from medication several days before the recording and in patients with no history of medication treatment. This suggests that the presence of beta oscillations in the STN-

GPI circuit is not solely attributable to medication and other factors besides drugs are involved in regulating neural activities in the circuit.

4.3. Couplings between the STN and GPI

The STN and GPI are connected via an excitatory projection from the STN to the GPI, which is integral to the indirect pathway of the cortico-basal ganglia circuit (Bolam et al., 2000). Previous studies have employed power synchronization, coherence, and phase-locking estimates to evaluate the connectivity between different regions within this circuit in dystonia and PD (Zhang et al., 2023; Fries, 2005; Neumann et al., 2015; Wang et al., 2018). In this regard, cortico-pallidal theta coherence has been reported to vary across delta and alpha frequency bands depending on whether the predominant symptoms are tonic or phasic (Yokochi et al., 2018). In our study, the negative correlation between theta phase coupling and clinical severity underscores the importance of regulating subthalamic-pallidal circuit to complement the suppression of pallidal theta power during DBS therapy.

Moreover, we found a significant negative correlation between clinical scores and power coupling in beta band (16–24 Hz). High-beta oscillation has been proposed as a distinct activity linked to signal transmission from the cortex to the STN via the hyperdirect pathway (Oswal et al., 2016; Oswal et al., 2021). In PD, pathological low-beta oscillation in the indirect pathway and cortico-subcortical coherence are provoked by high-beta oscillation (Oswal et al., 2016). In dystonia, a magnetoencephalography study also reported cortical driven cortico-pallidal beta coherence (Neumann et al., 2015), and a connectome study demonstrated that the dysfunctional network of dystonia is primarily characterized by connections between sensorimotor cortices and the STN (Hollunder et al., 2024). This suggests that beta activity may involve in imbalance between direct and indirect pathways and through the hyperdirect pathway, ultimately leading to hyperkinetic dystonia.

4.4. Considerations for DBS in dystonia

Pallidal theta power has been regarded as a potential pathophysiological marker since high-frequency DBS can suppress theta power and pallidal-cortical coherence in cervical dystonia patients (Barow et al., 2014). However, a study attempting to use it as feedback for closed-loop DBS revealed no significant differences in oscillatory power or acute symptom alleviation across stimulation conditions, including pseudo-stimulation, continuous DBS, and closed-loop DBS (Pina-Fuentes et al., 2020). Our findings indicate that a combination of selected features within the STN-GPI circuit can reflect clinical severity and the improvements of DBS treatment, whereas pallidal theta power alone may not be sufficient. A recent study showed that STN-DBS for dystonia does not specifically suppress theta power but rather broadly suppresses subthalamic power over 25–80 Hz, comparable to observations in PD (Wiest et al., 2023). The controversy surrounding the effectiveness of DBS in alleviating dystonic symptoms through suppressing theta activity necessitates more holistic research beyond the scope of pallidal theta oscillations. Our results indicate that the subthalamic beta power and the STN-GPI couplings, including beta power coupling and theta phase coupling, significantly contribute to the clinical scores. This finding suggests that, when developing novel strategies for DBS in the treatment of dystonia, we should maintain an open mind and consider the multiple oscillatory activities occurring within the circuit, as well as the dynamic interactions between the STN and GPI. This may require the application of GPI-DBS, STN-DBS, or a combination tailored to individual patient needs, with careful selection of appropriate markers for modulating different targets.

4.5. Limitations

Data acquisition was performed within 3–5 days postoperatively, with DBS activated for several days before the recording, necessitating

the consideration of potential stun effects and poststimulation effects. The patients included in the study had varied symptomatic phenotypes, which could potentially impact group-level statistical outcomes. Nonetheless, in our cohort, comparisons between the subgroup with cranial dystonia or cervical/generalized dystonia showed no significant difference in spectral power (see **Supplementary Fig. 1**). Despite being limited by the number of cases, preventing a more reliable detailed analysis, the current results still provide us with some insights to rethink the pathophysiological mechanisms of dystonia. Further comparisons and explorations of different phenotypes can be carried out by accumulating the number of cases.

5. Conclusions

We demonstrate in this study that theta and beta oscillations and their couplings within the STN and GPI circuit can reflect the severity of dystonia and DBS improvements. Beyond focusing on pallidal theta oscillations, acknowledging the significance of beta oscillations and STN-GPI couplings is essential for a more comprehensive exploration of the pathophysiology of dystonia and the development of optimal DBS strategies.

Funding sources

S.W. is supported by the Sci-Tech Innovation 2030 Agenda (No. 2021ZD0200407). X.G. is supported by the National Natural Science Foundation of China (No. 81901153), the Sci-Tech Innovation 2030 Agenda (No. 2022ZD205300), the National Key Research and Development Program of China (No.2021YFF1200605). G.Z. and J.Z. are supported by the National Natural Science Foundation of China (No. 81830033; No. 82171442; No. 81870888). Y.N. is supported by the National Natural Science Foundation of China (No. 82201400) and China Postdoctoral Science Foundation (No. 2022TQ0071). L.H. is supported by the National Natural Science Foundation of China (No. 32071061) and Beijing Natural Science Foundation (JQ22018).

CRediT authorship contribution statement

Xinyi Geng: Writing – original draft, Visualization, Methodology, Investigation, Funding acquisition, Formal analysis, Data curation, Conceptualization. **Zhaoyu Quan:** Visualization, Formal analysis, Data curation. **Ruili Zhang:** Investigation, Data curation. **Guanyu Zhu:** Resources, Data curation. **Yingnan Nie:** Writing – review & editing, Funding acquisition, Data curation. **Shouyan Wang:** Resources, Funding acquisition. **Edmund Rolls:** Writing – review & editing. **Jianguo Zhang:** Resources, Funding acquisition, Data curation. **Li Hu:** Writing – review & editing, Supervision, Conceptualization.

Declaration of generative AI and AI-assisted technologies in the writing process

During the preparation of this work the author used ERNIE Bot (Baidu, China) in order to check grammar and improve language. After using this tool, the author reviewed and edited the content as needed and takes full responsibility for the content of the publication.

Declaration of competing interest

None.

Data availability

The data in this study are not publicly available according to the Data Sharing Policy of the Fund Committee which allows the data to be used for the current study and repositied offline only. The data are, however, available from the corresponding author upon reasonable request and

with a signed copy of statement to keep it offline and for personal use.

Acknowledgments

We want to thank all patients who participated and supported this study.

Appendix A. Supplementary data

Supplementary data to this article can be found online at <https://doi.org/10.1016/j.nbd.2024.106581>.

References

- Albanese, A., 2014. Deep brain stimulation for cervical dystonia. *Lancet Neurol.* 13 (9), 856–857.
- Albanese, A., et al., 2013. Phenomenology and classification of dystonia: a consensus update. *Mov. Disord.* 28 (7), 863–873.
- Barow, E., et al., 2014. Deep brain stimulation suppresses pallidal low frequency activity in patients with phasic dystonic movements. *Brain* 137, 3012–3024.
- Benjamini, Y., Hochberg, Y., 2018. Controlling the false discovery rate: a practical and powerful approach to multiple testing. *J. R. Stat. Soc. B. Methodol.* 57 (1), 289–300.
- Bolam, J.P., et al., 2000. Synaptic organisation of the basal ganglia. *J. Anat.* 196 (Pt 4), 527–542.
- Brittain, J.S., Brown, P., 2014. Oscillations and the basal ganglia: motor control and beyond. *NeuroImage* 85, 637–647.
- Brittain, J.-S., Sharott, A., Brown, P., 2014. The highs and lows of beta activity in cortico-basal ganglia loops. *Eur. J. Neurosci.* 39 (11), 1951–1959.
- Cagnan, H., Duff, E.P., Brown, P., 2015. The relative phases of basal ganglia activities dynamically shape effective connectivity in Parkinson's disease. *Brain* 138, 1667–1678.
- Chen, C.C., et al., 2006. Oscillatory pallidal local field potential activity correlates with involuntary EMG in dystonia. *Neurology* 66 (3), 418–420.
- Chou, K.L., et al., 2005. Bilateral subthalamic nucleus deep brain stimulation in a patient with cervical dystonia and essential tremor. *Mov. Disord.* 20 (3), 377–380.
- Cohen, M.X., 2014. *Analyzing Neural Time Series Data: Theory and Practice*. MITpress.
- Fries, P., 2005. A mechanism for cognitive dynamics: neuronal communication through neuronal coherence. *Trends Cogn. Sci.* 9 (10), 474–480.
- Geng, X., et al., 2017. Comparison of oscillatory activity in subthalamic nucleus in Parkinson's disease and dystonia. *Neurobiol. Dis.* 98, 100–107.
- Hollunder, B., et al., 2024. Mapping dysfunctional circuits in the frontal cortex using deep brain stimulation. *Nat. Neurosci.* 21 (3), 573–658.
- Kuehn, A.A., et al., 2008. Increased beta activity in dystonia patients after drug-induced dopamine deficiency. *Exp. Neurol.* 214 (1), 140–143.
- Lee, J.R., Kiss, Z.H.T., 2014. Interhemispheric difference of pallidal local field potential activity in cervical dystonia. *J. Neurol. Neurosurg. Psychiatry* 85 (3), 306–310.
- Liu, X., et al., 2006. Different mechanisms may generate sustained hyper tonic and rhythmic bursting muscle activity in idiopathic dystonia. *Exp. Neurol.* 198 (1), 204–213.
- Lofredi, R., et al., 2023. Pallidal Beta activity is linked to stimulation-induced slowness in dystonia. *Mov. Disord.* 38 (5), 894–899.
- Lopez-Azcarate, J., et al., 2010. Coupling between beta and high-frequency activity in the human subthalamic nucleus may be a pathophysiological mechanism in Parkinson's disease. *J. Neurosci.* 30 (19), 6667–6677.
- Marsden, C.D., Obeso, J.A., 1994. The functions of the basal ganglia and the paradox of stereotaxic surgery in Parkinson's disease. *Brain* 117 (Pt 4), 877–897.
- Moll, C.K.E., et al., 2014. Asymmetric pallidal neuronal activity in patients with cervical dystonia. *Front. Syst. Neurosci.* 8, 15.
- Muller, J., et al., 2004. Craniocervical dystonia questionnaire (CDQ-24): development and validation of a disease-specific quality of life instrument. *J. Neurol. Neurosurg. Psychiatry* 75 (5), 749–753.
- Neumann, W.-J., et al., 2015. Cortico-pallidal oscillatory connectivity in patients with dystonia. *Brain* 138, 1894–1906.
- Neumann, W.-J., et al., 2017. A localized pallidal physioma in cervical dystonia. *Ann. Neurol.* 82 (6), 912–924.
- Neumann, W.J., et al., 2019. Toward electrophysiology-based intelligent adaptive deep brain stimulation for movement disorders. *Neurotherapeutics.* 16 (1), 105–118.
- Ostrem, J.L., et al., 2011. Subthalamic nucleus deep brain stimulation in primary cervical dystonia. *Neurology* 76 (10), 870–878.
- Oswal, A., et al., 2016. Deep brain stimulation modulates synchrony within spatially and spectrally distinct resting state networks in Parkinson's disease. *Brain* 139, 1482–1496.
- Oswal, A., et al., 2021. Neural signatures of hyperdirect pathway activity in Parkinson's disease. *Nat. Commun.* 12 (1), 5185.
- Pina-Fuentes, D., et al., 2018. The characteristics of pallidal low-frequency and beta bursts could help implementing adaptive brain stimulation in the parkinsonian and dystonic internal globus pallidus. *Neurobiol. Dis.* 121, 47–57.
- Pina-Fuentes, D., et al., 2020. Low-frequency oscillation suppression in dystonia: implications for adaptive deep brain stimulation. *Parkinsonism Relat. Disord.* 79, 105–109.
- Romito, L.M., et al., 2013. Long-term follow-up of GPi deep brain stimulation in generalized dystonia: primary dystonia compared to cerebral palsy. *Mov. Disord.* 28, S434.
- Scheller, U., et al., 2019a. Pallidal low-frequency activity in dystonia after cessation of long-term deep brain stimulation. *Mov. Disord.* 34 (11), 1734–1739.
- Scheller, U., et al., 2019b. Pallidal low-frequency activity in dystonia after cessation of long-term deep brain stimulation. *Mov. Disord.* 34 (11), 1734–1739.
- Schjerling, L., et al., 2013. A randomized double-blind crossover trial comparing subthalamic and pallidal deep brain stimulation for dystonia clinical article. *J. Neurosurg.* 119 (6), 1537–1545.
- Susatia, F., et al., 2010. An evaluation of rating scales utilized for deep brain stimulation for dystonia. *J. Neurol.* 257 (1), 44–58.
- Vinck, M., et al., 2011. An improved index of phase-synchronization for electrophysiological data in the presence of volume-conduction, noise and sample-size bias. *NeuroImage* 55 (4), 1548–1565.
- Wang, D.D., et al., 2016. Subthalamic local field potentials in Parkinson's disease and isolated dystonia: an evaluation of potential biomarkers. *Neurobiol. Dis.* 89, 213–222.
- Wang, D.D., et al., 2018. Pallidal deep-brain stimulation disrupts Pallidal Beta oscillations and coherence with primary motor cortex in Parkinson's disease. *J. Neurosci.* 38 (19), 4556–4568.
- Weinberger, M., et al., 2012. Oscillatory activity in the globus pallidus internus: comparison between Parkinson's disease and dystonia. *Clin. Neurophysiol.* 123 (2), 358–368.
- Welch, P., 1967. The use of fast Fourier transform for the estimation of power spectra: a method based on time averaging over short, modified periodograms. *IEEE Trans. Audio Electroacoust.* 15 (2), 70–73.
- Wiest, C., et al., 2023. Subthalamic nucleus stimulation-induced local field potential changes in dystonia. *Mov. Disord.* 38 (3), 423–434.
- Xie, H., et al., 2024. Deep brain stimulation of the subthalamic nucleus for primary Meige syndrome: clinical outcomes and predictive factors. *J. Neurosurg.* 1–14.
- Yokochi, F., et al., 2018. Resting-state Pallidal-cortical oscillatory couplings in patients with predominant phasic and tonic dystonia. *Front. Neurol.* 9, 375.
- Zhang, H., et al., 2020. A multi-sensor wearable system for the quantitative assessment of Parkinson's disease. *Sensors (Basel)* 20 (21).
- Zhang, R., et al., 2023. Balance between pallidal neural oscillations correlated with dystonic activity and severity. *Neurobiol. Dis.* 183, 106178.
- Zhu, G., et al., 2018. Characteristics of Globus pallidus internus local field potentials in hyperkinetic disease. *Front. Neurol.* 9, 934.